*Thermochimica Acta*, 145 (1989) 33–49
Elsevier Science Publishers B.V., Amsterdam – Printed in The Netherlands


# CHARACTERISTICS OF MARINE FERROMANGANESE CONCRETIONS AT ELEVATED TEMPERATURE

B.K. MOHAPATRA, S.K. MISHRA and R.K. SAHOO
*Regional Research Laboratory, Bhubaneswar, Orissa (India)*
(Received 18 July 1988)

## ABSTRACT

The characteristics of ferromanganese concretion samples of various morpho-chemistries at elevated temperatures have been investigated. These concretions have four unique physical properties such as high porosity, large surface area, high water content and ultrafine particle size. Dehydration of these samples around 150 °C strengthens oxides and silicates and the minerals become more crystalline. $\delta$-$MnO_2$ and todorokite form the predominant manganese mineral phases of which the latter collapses on heating at 120 °C. Crystalline phases of iron mineral appear only around 500 °C calcination. Because of the possible existence of non-crystalline hydrated ions, either as independent phase or as interlayer, within silicate minerals, these concretions lose weight continuously upon heating even above 800 °C. At higher temperature the higher oxides of manganese and iron phases reduce to their lower oxides and quartz gets adsorbed into the manganese/iron phase. The BET surface areas of all the samples show a gradual increase up to 300–400 °C followed by a sharp fall until 600 °C and ultimately reduce to zero at 800 °C calcination. Variation in water content and surface area, DTA-TG and XRD patterns between the two major ferromanganese concretions, viz. nodule and crust types, attest to a difference in their environment of deposition in the Indian Ocean basin.

## INTRODUCTION

The ferromanganese concretions of the ocean floor are a potential source of many valuable metals, such as cobalt, nickel, copper, manganese, etc. For extraction of these metals, the mode of occurrence and physical and textural characteristics of these concretions need to be well understood. Gaining metal values through pyrometallurgical process routes involves high temperature treatment. Hence it is also necessary to know possible changes of physicotextural properties and transformation of phases due to the effects of thermal treatment. Although physical properties and internal characteristics of marine nodules have been extensively studied [1], investigations on the effect of temperature on the physicochemical characteristics of manganese nodules have been attempted [2,3] with limited success. The present study aims to elucidate the physical characteristics of three types of ferro-

0040-6031/89/$03.50 

TABLE 1

Some physicochemical characteristics of ferromanganese concretions of the Indian Ocean

| Sample type | Chemical analysis (wt.%) | | | | | | Physical characteristics | | | |
|---|---|---|---|---|---|---|---|---|---|---|
| | $SiO_2$ | Mn | Fe | Cu | Ni | Co | Bulk density ($g\ cm^{-3}$) | Grain density ($g\ cm^{-3}$) | Porosity (%) | Specific surface area ($m^2\ g^{-1}$) |
| Nodule (F4/1) | 11.22 | 31.80 | 6.80 | 1.70 | 1.35 | 0.16 | 1.47 | 2.19 | 49 | 39 |
| Polynodule (F8/4) | 31.05 | 11.57 | 14.96 | 0.25 | 0.46 | 0.14 | 1.28 | 2.34 | 48 | 40 |
| Crust (F8/1) | 9.00 | 14.33 | 20.92 | 0.23 | 0.28 | 0.29 | 1.34 | 2.16 | 30 | 55 |

manganese concretion samples from the Central Indian Ocean basin, having different morpho-chemistries, and the effect of thermal treatment on their properties at elevated temperature.

## CHARACTERISTICS OF FERROMANGANESE CONCRETIONS

The ferromanganese concretions recovered from the Central Indian Ocean basin can be divided into three distinct morphologies: nodule, polynodule and crust; belonging respectively to three environmental sites: abyssal plain, hill slopes and sea mount region. These concretions have four outstanding physical properties (Table 1): high porosity (av. 42%), ultrafine grain size (av. 100 Å), high water bearing and large surface area. Mineralogically, nodule comprises todorokite and $\delta$-$MnO_2$, whilst polynodule comprises $\delta$-$MnO_2$ and minor todorokite and crust only $\delta$-$MnO_2$. Nodule is invariably rich in Mn, Cu and Ni; the crust is rich in Fe and Co while the polynodule has an intermediate composition (Table 1). Although the iron content in these concretions ranges between 4 and 21%, no distinct mineral phase is detected because of its cryptocrystalline or amorphous nature. However, the occasional presence of goethite/akaganeite has been recorded in one or two samples. The detrital quartz and feldspar content increases from crust to polynodule and nodule types. The presence of merlinoite (a zeolite mineral) has been reported [4] in nodule and polynodule types. Copper, nickel, cobalt, lead and zinc do not appear as independent mineral species, but instead occur in an adsorbed state within the manganese/iron phase.

## EXPERIMENTAL

The ferromanganese concretion samples characterised during the present investigation were dredged from the Central Indian Ocean basin during cruises of the Fernela 'F4' and 'F8' conducted by the National Institute of Oceanography, Goa, India.

Heat treatment of three samples (nodule, polynodule and crust) was carried out in a furnace maintained at $\pm 50\,^{\circ}C$. The furnace was first heated to the requisite temperature and 4–5 g of sample (200 mesh. B.S.) placed in a platinum crucible was introduced into the furnace. After 4 h of heating at different temperatures (120 °C, 400 °C, 600 °C and 800 °C) the sample was withdrawn and stored in a desiccator.

The various methods carried out to reveal the characteristics of these concretions at elevated temperature are as follows.

(i) To ascertain water loss, powder samples (150 mesh, B.S.) of each concretion type were heated for 4 h in an air oven at various temperatures and the mass losses were measured.

(ii) The surface area was evaluated by a low temperature (−196 °C) nitrogen adsorption method with the help of a high speed surface area analyser (Micrometric Instrument Corp., U.S.A., Model 2200).

(iii) For thermolysis (DTA, DTG and TG) a suitable amount (0.3–0.69 g) of powdered (200 mesh) sample in a ceramic crucible was subjected to heating in air up to a maximum temperature of 940 °C in a Derivatograph (MOM, Budapest). The heating rate was 10 °C $min^{-1}$. The sensitivities of TG, DTG and DTA were 500 mg, 1/10 and 1/10 respectively. $\alpha$-$Al_2O_3$ was used as the reference substance.

(iv) The XRD study was carried out by means of a Phillips diffractometer (PW-1400) having automatic divergence slit, receiving slit and graphite monochromator assembly. Cu $K\alpha$ radiation operating at 40 kV and 20 mA was used for this purpose.

(v) The IR spectra of the nodule sample only (up to 600 °C) was taken by the KBr matrix technique, using a Pye-Unicam IR spectrometer in the 4000–200 $cm^{-1}$ region.

## RESULTS AND INTERPRETATION

### *Water content*

One of the significant characteristics of ferromanganese concretions is their high water content. The large water-bearing capacity is due to their ultrafine grain size, high porosity and spongy nature. The concretion appears to lose mass continuously with rise in temperature (Table 2). A considerable proportion of water (about 20%) is lost at 120 °C. This loss is due to the hygroscopic water/free moisture content of the concretions. Although DTA curves of manganese nodule samples usually exhibit a peak temperature for moisture loss at 150–160 °C, it has been reported that drying for a longer period (> 4 h) at 120 °C gives the same loss of moisture. Some of the loss around 400 °C may be due to decomposition of structural water (dehydroxylation). At temperatures above 600 °C the mass loss is perhaps due to decomposition of oxide phases and also partly due to loss of

TABLE 2

Mass loss of ferromanganese concretions after heating for 4 h in a furnace

| Sample type | Mass loss at 120 °C | Mass loss at 400 °C | Mass loss at 600 °C | Mass loss at 800 °C | Mass loss at 1000 °C |
|---|---|---|---|---|---|
| Nodule | 16.50 | 21.53 | 27.83 | 30.56 | 30.92 |
| Polynodule | 15.80 | 20.96 | 23.54 | 27.52 | 28.49 |
| Crust | 22.15 | 33.36 | 37.35 | 41.57 | 42.20 |

volatiles. The gradual mass loss at elevated temperature has also been recorded from a series of thermogravimetric analyses.

*Porosity and surface area*

The other striking physical properties of ferromanganese concretion are its high porosity and surface area, which are a direct result of agglomeration of ultrafine colloidal particles in these concretions. The average particle size of the grains has been calculated to be 30–450 Å by Von Heimendahl [5] and 100 Å by Johnson and Glasby [6].

The porosities of the samples have been calculated from the bulk densities obtained from volume displacement in water using the formula

$$\text{Porosity} = \frac{W_2 - W_1}{W_2 - W_3} \times 100\%$$

where $W_1$ is the mass of the sample, $W_2$ is the mass of the water saturated sample and $W_3$ is the mass of the sample under immersion.

Pores within nodules possess a distribution of diameters, which extend from the micron size down to a few angstroms. Han et al. [2] calculated the average pore diameter of the nodule to be approximately 80–150 Å. In general, nodules have higher porosity (49%) than polynodules (48%) and crust (40%). No relation exists between density or porosity of these concretions and their chemistry (Table 1).

Change of surface area of ferromanganese concretions as a function of temperature was investigated and the results are listed in Table 3 and illustrated in Fig. 1. The results show that the surface area of nodule and polynodule types appears to increase upon heating to 400 °C, while in the crust sample surface area increases upon heating to 300 °C. The surface

TABLE 3

Change of surface area versus temperature

| Heat treatment (°C) | Surface area ($m^2\ g^{-1}$) | | | |
|---|---|---|---|---|
| | Pacific Ocean nodule [2] | Marine concretions of Indian Ocean | | |
| | | Nodule | Polynodule | Crust |
| Room temperature (mass basis) | – | 39 | 40 | 55 |
| 25– 50 | 205 | 24.1 | 24.7 | 44 |
| 110–120 | 300 | 39.3 | 103.8 | 52 |
| 300 | – | 52.2 | 115 | 146 |
| 400 | 86 | 59 | 118.7 | 71.1 |
| 500 | – | 22.2 | 59.4 | 27.4 |
| 600 | 13.5 | 7.2 | 13 | 5 |
| 800 | 2.2 | 0 | 0 | 0 |

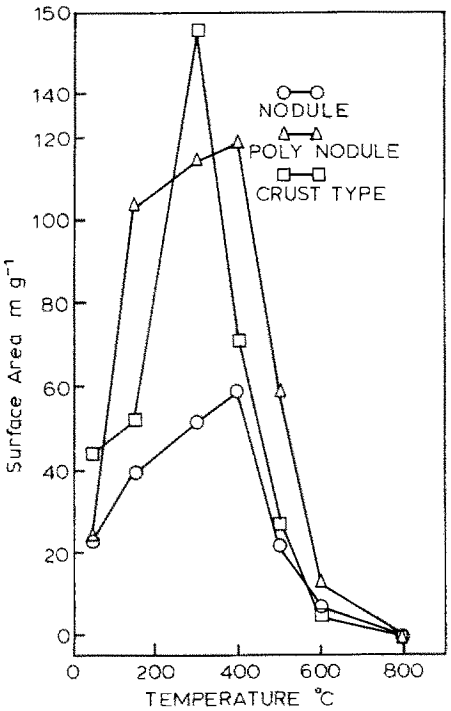


Fig. 1. Plot showing surface area versus temperature in different ferromanganese concretion samples.

areas of all these samples decrease as the temperature is raised further and ultimately reduce to zero at 800 °C. Similar behaviour concerning the decrease of surface area upon heating was observed by Weisz [7] and Fuerstenau and Han [3].

*Thermal analysis*

All three types of concretion were subjected to thermal analysis (DTA, TG and DTG) and the results are illustrated in Fig. 2 (A,B,C) and Table 4: nodule and polynodule show very similar behaviour on heating.

*Nodule and polynodule types*

DTA curves show four endothermic peaks at 160 °C, 460 °C, 640 °C and 865 °C for the nodule sample and four endothermic peaks at 150 °C, 460 °C, 650 °C and 870 °C for the polynodule sample. These reactions occur at the points near the changes in shape of TG and DTG curves. The total mass loss at 910 °C was found to be 22.78% for the nodule type and 20.94% for polynodule type (Fig. 2A,B).

Thermogravimetric analyses of both samples exhibit sharp mass loss between 50 °C and 300 °C (12–14%) and a DTA peak at 160–150 °C; the

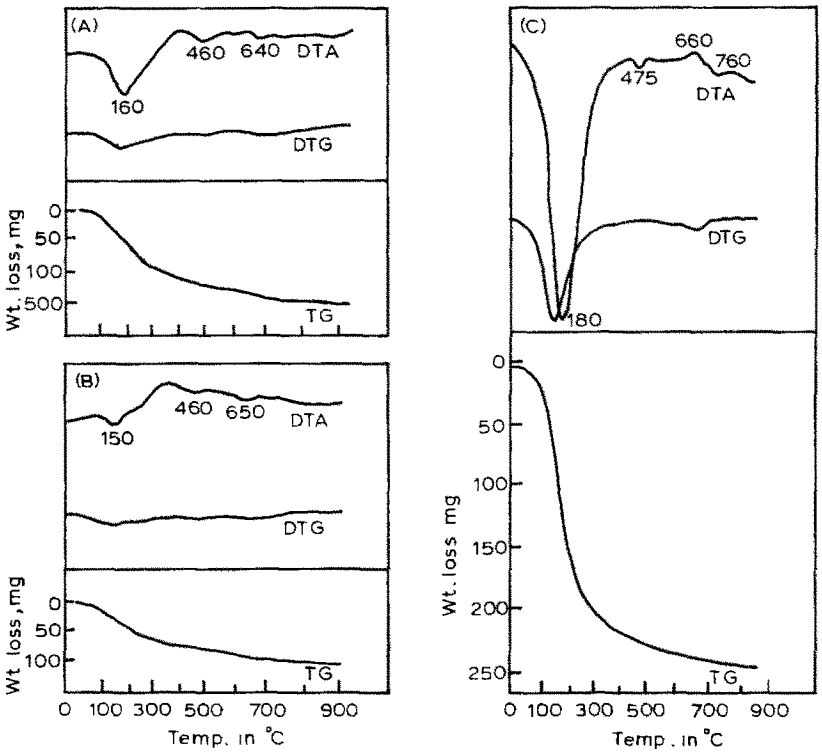


Fig. 2. DTA, TG and DTG thermograms for manganese nodule (A); polynodule (B) and ferromanganese crust (C) samples.

samples lose about 5–7.5% of their mass due to dehydration. The mass loss of 3.7–4.1% between 300 °C and 480 °C with a second endothermic peak (460 °C) is due to loss of structural water (dehydroxylation) from hydrous iron oxide ($FeOOH \rightarrow Fe_2O_3$) and hydrous aluminosilicate phases. Between 480 °C and 700 °C, the samples lose 3.1–3.7% of their mass and this loss is characterised by a broad endothermic peak (640–650 °C) mainly due to the conversion of $MnO_2$ to $Mn_2O_3$ with escape of oxygen (oxygenation). Final mass loss (1.2–1.6%) takes place at a slower rate with the last endotherm at 865–870 °C most probably being due to conversion of $Fe_2O_3$ to $Fe_3O_4$ and $Mn_2O_3$ to $Mn_3O_4$. Han et al. [2], however, reported strong endothermic reactions around 200 °C, 450 °C and 650 °C in the case of a $\delta$-$MnO_2$ rich nodule sample.

*Crust type*

The illustration in Fig. 2C is the thermogram of ferromanganese crust sample (F 8/1) obtained on heating. The DTA curve shows three endothermic peaks at 180 °C, 470 °C and 700 °C and two exothermic peaks at 660 °C and 760 °C. Two endothermic reactions and one exothermic reaction

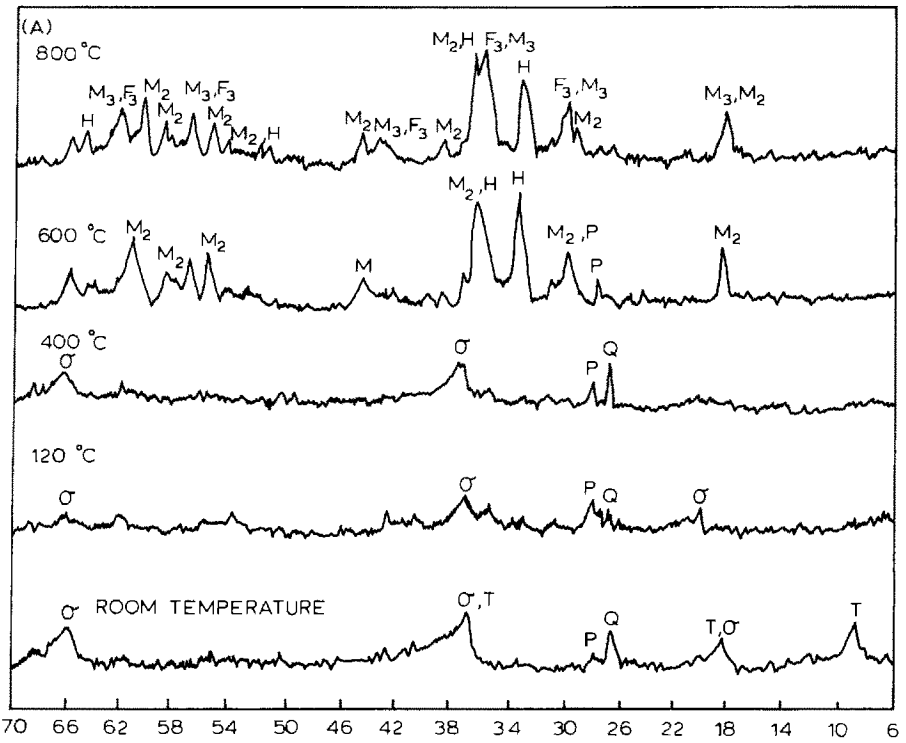
(A)
800 °C
600 °C
400 °C
120 °C
ROOM TEMPERATURE
70 66 62 58 54 50 46 42 38 34 30 26 22 18 14 10 6

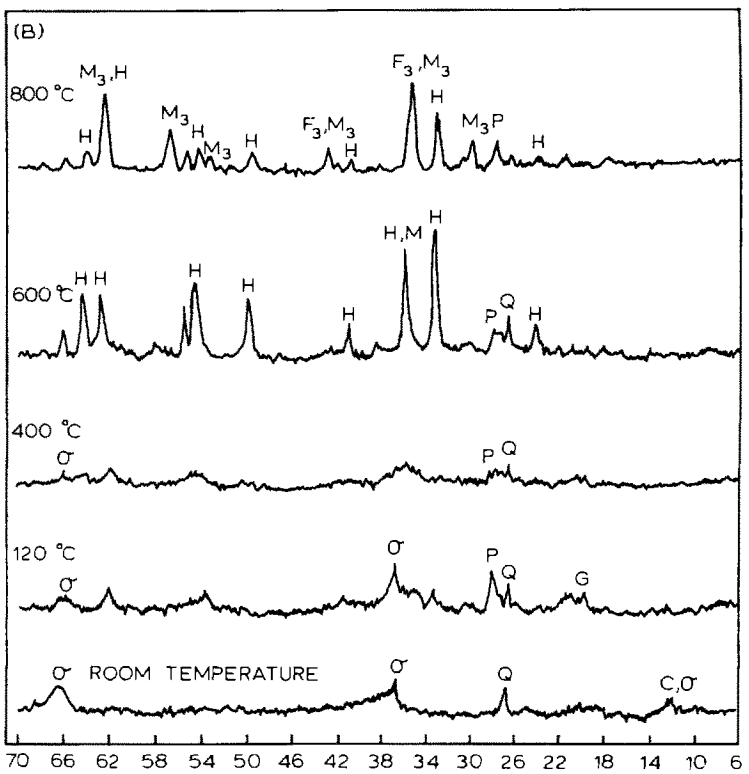
(B)
800 °C
600 °C
400 °C
120 °C
ROOM TEMPERATURE
70 66 62 58 54 50 46 42 38 34 30 26 22 18 14 10 6

occur at the point near the changes in shape of TG curves. DTG peaks however, show minor shifts corresponding to DTA peaks. The total mass loss in this sample is 34.60% at the maximum temperature of 840 °C, which is far above the nodule and polynodule types.

The sample loses about 30% of its mass between 60 °C and 380 °C due to release of hygroscopic moisture, with the most prominent and sharp endothermic peak at 180 °C, the maximum mass loss of 18.9% being attained at the same peak temperature. Between 380 °C and 640 °C, the sample slowly loses 3.2% of its mass and exhibits one small, sharp endothermic peak at 470 °C because of the decomposition of hydrous oxides of iron ($FeOOH \rightarrow Fe_2O_3$). 1.4% of mass loss between 640 °C and 840 °C is due to escape of oxygen and other volatiles. The exothermic peaks at 660 °C and 760 °C are very probably due, respectively, to phase transformation of $\alpha$-$Fe_2O_3$ to $\gamma$-$Fe_2O_3$ and $\alpha$-$Mn_2O_3$ to $\gamma$-$Mn_2O_3$. The medium magnitude endotherm at 700 °C may be due to decomposition of $\delta$-$MnO_2$ to $\alpha$-$Mn_2O_3$ (?).

*X-Ray diffraction analysis*

The X-ray diffraction analyses of manganese and crust types were obtained under similar instrumental settings for both original samples and their respective calcined products and are illustrated in Fig. 3A,B. Polynodule types exhibit similar patterns to those of nodule types, and hence are not reported separately.

As can be seen from Fig. 3 at room temperature, the nodules exhibit characteristic peaks of two manganese minerals such as todorokite (9.8 Å, 4.80 Å) and $\delta$-$MnO_2$ (Fig. 3A), whilst two very diffuse and weak peaks at the *d*-spacings of 2.41 Å and 1.41 Å, diagnostic of $\delta$-$MnO_2$, appear in ferromanganese crust (Fig. 3B). Iron, which is present in considerable proportion in both nodule and crust samples, does not exhibit any defined peaks because of its very poorly crystalline or amorphous nature. In the silicate mineral group, the sharp diagnostic diffraction line (3.32 Å) of quartz ($\alpha$-$SiO_2$) appears in both sample types. A very weak reflection of plagioclase/zeolite mineral (3.18 Å) appears in the nodule sample, whilst only traces of clay mineral (7.2 Å) are recorded in crust type.

Heating of nodule at around 120 °C for 4 h showed that the todorokite phase breaks down near that temperature without development of any new

Fig. 3A. X-ray diffraction pattern of ferromanganese nodule sample calcined at different temperatures. (T-Todorokite, $\delta$-$\delta$-$MnO_2$, Q-Quartz, P-Feldspar, $M_2$-$Mn_2O_3$, $M_3$-$Mn_3O_4$, H-Hematite '$Fe_2O_3$',$F_3$-$Fe_3O_4$).

Fig. 3B. X-ray diffraction pattern of ferromanganese crust sample calcined at different temperatures. ($\delta$-$\delta$-$MnO_2$, Q-Quartz, C-Clays, P-Feldspar, H-Hematite '$Fe_2O_3$', $F_3 = Fe_3O_4$, $M_2$-$Mn_2O_3$, $M_3$-$Mn_3O_4$).

TABLE 4

TG data from the decomposition of different types of ferromanganese concretions

| Sample type | TG loss (%) at various temperatures in different stages | | | | | | | | Total mass loss (%) |
|---|---|---|---|---|---|---|---|---|---|
| | Stage I | | Stage II | | Stage III | | Stage IV | | |
| | Temperature range (°C) | Mass loss (%) | Temperature range (°C) | Mass loss (%) | Temperature range (°C) | Mass loss (%) | Temperature range (°C) | Mass loss (%) | |
| Nodule | 50–290 | 14.1 | 290–480 | 3.7 | 480–700 | 3.7 | 700–920 | 1.2 | 22.78 |
| Polynodule | 50–300 | 12.0 | 300–480 | 4.1 | 480–700 | 3.1 | 700–920 | 1.6 | 20.94 |
| Crust | 60–380 | 30 | 380–640 | 3.2 | 640–840 | 1.4 | – | – | 34.60 |

minerals. Ostwald and Dubrawski [8] recorded that heating marine 10 Å manganate (similar as todorokite) to 100 °C for 4 h results in the formation of birnessite (7.0 Å). Collapse of this structure however, was found to be irreversible. In the case of the crust sample, the characteristic peak of $\delta$-$MnO_2$ becomes stronger because of dehydration and improved crystallinity. A very minor reflection characteristic of goethite (4.19 Å) occasionally appears in crust samples. Amongst silicate minerals, the relative intensity of quartz falls and the diffraction line of plagioclase/zeolite becomes stronger in nodule samples, whilst the minor reflection of clay minerals in ferromanganese crust disappears at 120 °C because of dehydration.

Nodule calcined around 400 °C showed its $\delta$-$MnO_2$ peaks becoming stronger because of improved crystallinity, whilst in ferromanganese crust these peaks become broad and weak. The reflection peak of quartz gets stronger whilst the plagioclase/zeolite line does not show any change in nodules. By contrast, in crust samples the quartz line does not show any change and the plagioclase peak shows a fall in intensity. The iron phase does not appear in any of these concretions at 400 °C heating.

Calcination around 600 °C results in the appearance of strong XRD peaks at 2.69 Å and 1.69 Å indicating the existence of iron phase hematite ($\alpha$-$Fe_2O_3$) in both samples. This phase develops during heating from a phase transformation of amorphous oxyhydroxide ($\alpha$-FeOOH). The higher peak intensity of $\alpha$-$Fe_2O_3$ in crust, compared to that of nodule samples, clearly indicates the relative abundance of iron in the former type. Around this temperature $\delta$-$MnO_2$ also decomposes to $\gamma$-$Mn_2O_3$ as indicated by the appearance of a distinctive line at 2.49 Å in both samples. The preponderance of the manganese phase in nodule over that of crust sample is brought out at this temperature by the appearance of a strong diffraction line at 4.87 Å in the former. The diffraction line of quartz in nodule disappears at 600 °C, probably because of its adsorption into the manganese/iron phase. By contrast in ferromanganese crust these lines become stronger at this temperature.

When the ferromanganese concretion is heated in air for 4 h at a temperature around 800 °C, a distinct and sharp reflection line appears at 2.53 Å which corresponds to that of $Mn_3O_4$ and $Fe_3O_4$. Previous workers [2,9] have recorded the decomposition of todorokite to $Mn_3O_4$ between 600 °C and 625 °C. In the case of nodules at this temperature both $Mn_3O_4$ and $Fe_3O_4$ seem to be present in equal proportion with subordinate amounts of $Fe_2O_3$ and $Mn_2O_3$. As the various *d*-spacing values of both $Mn_3O_4$ and $Fe_3O_4$ standards are very similar [10], the presence of $Fe_3O_4$ (magnetite) phase was confirmed as the calcined products of both the sample types were found to be highly magnetic. In crust sample, the conversion of $Mn_2O_3$ to $Mn_3O_4$ is recorded with the presence of minor $Fe_2O_3$ and $Fe_3O_4$ phases. At this temperature the plagioclase peak disappears in the nodule sample but remains in the crust sample.

*Infrared analysis*

Ultrafine grain size and poor crystallinity of mineral constituents in ferromanganese concretions often give ambiguous XRD results. In such cases IR spectral analysis is quite useful because of its sensitivity to short range order. Limited attempts have been made [11,12] in the past to use IR spectroscopy for investigating marine nodules.

IR spectral analysis results of different calcined products (120 °C, 200 °C, 400 °C and 600 °C) of nodule samples only are illustrated in Fig. 4. The products heated at 800 °C could not be exposed because of instrumental problems. The changes observed from higher wavenumbers towards lower wavenumbers as the temperature is elevated are discussed below.

The drying of bulk nodule sample at 120 °C results in the appearance of a number of weak absorption bands in the 3700–3000 $cm^{-1}$ region, generally assigned to OH vibration. Hence after removal of adhering moisture, the hydrated minerals become more crystalline or more ordered in their lattice position. At higher temperature (600 °C) this vibration is shifted from 3420 $cm^{-1}$ to 3460 $cm^{-1}$. This shift may be ascribed to release of both adsorbed and molecular water.

At 200 °C calcination, many of the peaks either disappear or exhibit much lower intensity, indicating considerable loss of $H_2O$ from lattice positions. Since OH groups are more strongly bonded to the lattice than $H_2O$ molecules, distinct peaks in the 4000–3700 $cm^{-1}$ region indicate

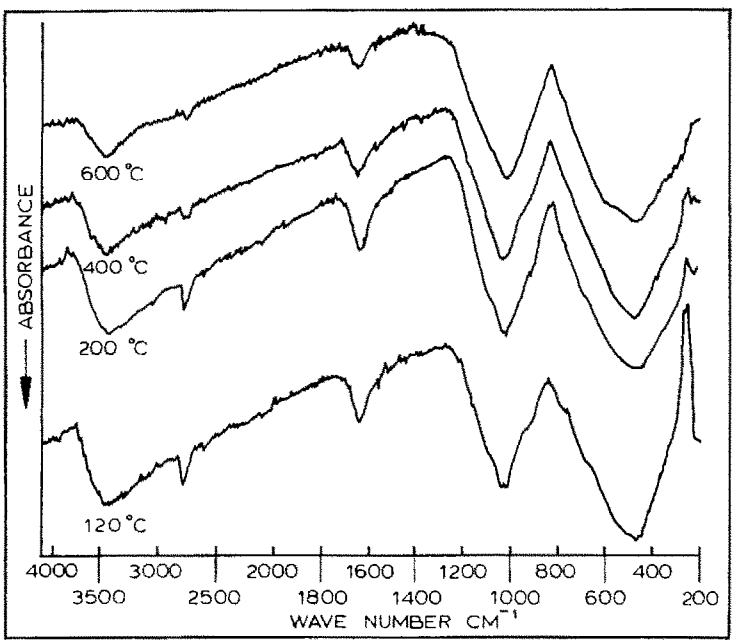


Fig. 4. Infrared spectra of manganese nodule sample calcined at different temperature.

various hydrogen bonded OH groups with surface oxygen in clay minerals and probably also zeolites.

The intensity of the sharp peak at 2790 $cm^{-1}$ gradually decreases on heating and at 400 °C calcination it disappears and a doublet appears at 2760–2720 $cm^{-1}$. This peak is probably due to iron oxyhydroxide (akaganeite) which undergoes dehydroxylation around 400 °C. This oxyhydroxide of iron exhibits a sharp doublet at 2800–2900 $cm^{-1}$ [13]. In addition, crystallographically different Mn–OH bands sometimes show more than one absorption band in the 2600–2800 $cm^{-1}$ region [14]. On calcination in air MnOOH undergoes oxidation to $MnO_2$ and this takes place in the temperature range 350–400 °C. In the present case also, the intensity of peaks in this region gradually decreases on calcination up to 400 °C.

Structural water bending vibration was observed at 1640 $cm^{-1}$. The intensity of this vibration gradually gets much weaker as the temperature rise. Potter and Rossman [15] ascribed sharp bands in the 1600–1700 $cm^{-1}$ region to todorokite-rich manganese ore. The present authors however found from XRD studies that the todorokite structure is very unstable and collapses upon heating at 120 °C. Hence we attribute this band to some iron oxyhydroxide mineral (FeOOH) which gradually transforms to $Fe_2O_3$ at elevated temperatures.

Nodules, in general, exhibit very strong absorption in the 1035–1020 $cm^{-1}$ region. This band is usually broadened by about 50–60 $cm^{-1}$ and is due to Si–O or Si–O–Al vibration in both silicate and aluminosilicate minerals. The shortening of this band at 200 °C and 400 °C indicates that the silicates become more crystalline. Moreover, further broadening of this absorption in this region at 600 °C calcination indicates lattice disorder in the Si–O stretching vibration associated with these silicates.

As the temperature rises the shoulder at 925 $cm^{-1}$ gets shifted towards lower frequencies and finally disappears at 600 °C. Some investigators [11] have assigned this absorption to the out-of-plane bending mode of hydrous manganese mineral. It may also be due to Al–Al–OH liberation in smectite type minerals [16]. The dehydroxylation of hydrous manganese minerals or clay minerals is evident from the disappearance of this band at higher temperatures.

The weak doublet at 780–805 $cm^{-1}$ is characteristic of quartz [17] which is a common associate in nodule samples. On calcination this doublet gradually converges to one peak at 810 $cm^{-1}$ and finally disappears around 600 °C. Probably at this temperature quartz gets adsorbed into the manganese/iron phase.

The appearance of a distinct shoulder at 520 $cm^{-1}$ when the sample is calcined at 600 °C can perhaps be ascribed to conversion of higher oxides of manganese ($MnO_2$) to lower oxides of manganese ($Mn_2O_3$).

Liberational modes due to rotational oscillation of uncoordinated water may account for some of the bands in the region below 600 $cm^{-1}$. In the

present sample, the fact that the band at 275 $cm^{-1}$ gets weaker on initial heating at 100 °C may account for uncoordinated water. Some of the bands in this region are also due to metal–oxygen stretching. However, the IR absorption peaks in the 500–200 $cm^{-1}$ region remain broadly unchanged on heating and therefore are not related to structural water. Farmer [18] assigned absorptions at 460 $cm^{-1}$ and 430 $cm^{-1}$ as being typical of smectite type clay minerals while some others [15] suggest absorption at 430–440 $cm^{-1}$ to be due to Mn–O vibrations in birnessite and todorokite.

## DISCUSSION

The characteristic changes obtained at elevated temperature in respect of physical, textural and mineralogical properties of marine ferromanganese concretions have been investigated using various techniques including surface area, DTA-TG, XRD and IR analysis.

An outstanding property of ferromanganese concretions is the presence of physically and chemically adsorbed water. The water molecules which condense in micropores due to capillary action evaporate continuously at higher temperatures.

The result of the effect of heat treatment on the surface area indicates that for nodule and polynodule samples it increases from 40 $m^2\ g^{-1}$ at room temperature to 118 $m^2\ g^{-1}$ at 400 °C and then gradually decreases as the temperature rises. In contrast, the crust sample maintains a trend showing an increase in surface area (146 $m^2\ g^{-1}$) only up to 300 °C and then follows a pattern similar to that of nodules. The fall after 400–300 °C is so sharp that at 600 °C the area is reduced to between 5 and 13 $m^2\ g^{-1}$. Beyond this temperature the surface area slowly falls and becomes zero at 800 °C. The surface area in these samples rises as they become free of hygroscopic moisture. The fall in surface area at high temperature is very probably due to phase transformation and the destruction of micropores. These irregular pores change to closed spherical mesopores due to internal sintering bringing about greater homogeneity. The surface area reducing to zero at 800 °C clearly reveals the complete close down of internal pores. Han et al. [2] have reported that at high temperature the small pores coalesce to give rise to larger ones and as a consequence, the average pore size decreases with time and the specific area also decreases but the total porosity remains virtually unchanged.

The thermal analysis of concretions highlights a distinct difference between ferromanganese nodules and encrustations. The major difference between them is their hygroscopic moisture content and total thermogravimetric loss (crust > nodule). The mass losses obtained at different temperatures in an air oven are more than those observed by DTA and TG studies, because a longer period of heating at a particular temperature in the former

case results in more mass loss than that recorded by a thermoanalytical instrument at the heating rate of 10 °C $min^{-1}$. The results also show that on prolonged heating the Mn–Fe phases in ferromanganese concretions, irrespective of their morphological variations, undergo crystalline modification. The degree of loss due to oxygenation and decomposition of iron and manganese phases into the final product of $Fe_3O_4$ and $Mn_3O_4$ phases was found to be higher in nodules, while phase transformation of $\alpha$-$Fe_2O_3$ to $\gamma$-$Fe_2O_3$ and $\alpha$-$Mn_2O_3$ to $\gamma$-$Mn_2O_3$ is well depicted by the strong exothermic peaks at 660 °C and 760 °C respectively in the crust sample. The results obtained from XRD studies show that the marine todorokite is very unstable and collapses upon heating around 120 °C without formation of any new minerals. $\delta$-$MnO_2$, the major manganese phase, does not exhibit any change upon heating up to 400 °C. With a higher degree of calcination, the $\delta$-$MnO_2$ decomposes to $\gamma$-$Mn_2O_3$ (> 600 °C) and $Mn_3O_4$ (800 °C). Iron, which lacks X-ray diffraction at room temperature, appears only upon heating to above 500 °C as the $\alpha$-$Fe_2O_3$ phase. This phase changes to $Fe_3O_4$ at 800 °C calcination resulting in a highly magnetic product. The XRD peaks diagnostic of silicates such as quartz and feldspar in nodules get stronger during heating due to improved crystallinity. The disappearance of these silicates above 600 °C is probably because of their adsorption into the manganese/iron phase. The clay mineral present in ferromanganese crust in scarce amounts disappears at 120 °C because of dehydration, and quartz disappears at 600 °C because of adsorption. However, the feldspar peaks in the crust sample appear throughout with minor variation in their intensity.

The IR study has revealed that dehydration of adsorbed water strengthens oxides and silicate phases in ferromanganese concretion samples and minerals become more crystalline. The structural water does not get completely released even at 600 °C calcination, indicating the possible existence of non-crystalline hydrated ions, either as an independent phase or as an interlayer within silicate minerals. At elevated temperature (600 °C) the higher oxides of the manganese phase change to their lower oxides and quartz gets adsorbed into the manganese/iron phase.

Summarising the results obtained from various techniques, it can be said that at elevated temperature the characteristics of marine ferromanganese concretions changes significantly. The changes recorded in nodules are different from those of ferromanganese crust samples, thereby indicating a difference in their depositional environment. This indirectly supports earlier workers [19–21] who have reported a variation in mechanism of formation between nodule and crust: the marine nodules are the product of diagenetic processes [19] resulting in growth of authigenic manganese minerals at sea water/sediment interface in the abyssal plains while the crust types occur over ridges and sea mounts due to accretion of material by hydrogenous precipitation of colloidal oxyhydroxide from normal sea water under a highly oxidising environment [20,21].

## CONCLUSIONS

The significant characteristics of marine ferromanganese concretions at elevated temperatures are as follows:

(1) Prolonged heating results in strengthening of the oxides and silicate phases in ferromanganese concretions and the minerals become more crystalline. Some minerals collapse at low temperature (120 °C) while some new minerals form at higher temperature.

(2) At elevated temperature the loss due to hydroscopic moisture is considerably more in ferromanganese crust samples (30%) as compared to other nodular types.

(3) The surface area of these concretions rises as the temperature increases up to 300–400 °C and then shows a fall. Amongst the concretion types, the surface area of crust sample rises to a maximum (146 $m^2\ g^{-1}$).

(4) The concretion samples gradually lose mass as the temperature rises above 800 °C calcination because of the existence of non-crystalline hydroxyl ions either as an independent phase condensed within agglomerated ultrafine particles or interlayered within the silicate minerals.

(5) The silicate minerals, especially quartz, in these concretions get adsorbed into manganese/iron phases at higher temperature (600 °C) and the higher oxides of manganese and iron reduce to their lower oxides.

Summarising, it may be concluded that heating various types of concretion brought out significant differences between two species, viz. nodule and crust types, concerning the dehydration–surface area domain and thermolysis–XRD pattern, thereby revealing a difference in their environments of deposition in the Central Indian Ocean basin.

## ACKNOWLEDGEMENTS

The authors are grateful to the Director, Regional Research Laboratory (RRL), Bhubaneswar for his kind permission to publish this paper. They also wish to record their thanks to the authorities of the Department of Ocean Development, Govt. of India, New Delhi who have sponsored the project and the National Institute of Oceanography, Goa who have provided the samples. Thanks are also due to Dr. S.B. Kanungo, Dr. J. Rajgopal Rao and Dr. B.S. Acharya, scientists of RRL for carrying out thermal, surface area and XRD analyses respectively.

## REFERENCES

1 G.P. Glasby, Marine Manganese Deposits, Elsevier, Amsterdam, 1977.
2 K.N. Han, M.P. Hoover and D.W. Fuerstenau, Mar. Min., 2 (1979) 139.

3 D.W. Fuerstenau and K.N. Han, Miner. Proc. Tech. Rev., 1 (1983) 1.
4 B.K. Mohapatra and R.K. Sahoo, Mineral. Mag., 51 (1987) 749.
5 M. Von Heimendahl, G.L. Hurbred, D.W. Fuerstenau and G. Thomas, Deep Sea Res., 23 (1976) 69.
6 C.E. Johnson and G.P. Glasby, Nature (London), 222 (1968) 371.
7 P.B. Weisz, J. Catal., 10 (1968) 407.
8 J. Ostwald and J.V. Dubrawski, Mineral. Mag., 51 (1987) 463.
9 C. Frondel, U.B. Marrin and J. Ito, Am. Mineral., 45 (1960) 1167.
10 JCPDS Data Book, 1980.
11 H. Elderfield and G.P. Glasby, Chem. Geol., 11 (1973) 117.
12 E.A. Perseil and C. Jehanno, Mineral. Deposita, 16 (1981) 391.
13 E. Murad, Clay Miner., 14 (1979) 273.
14 Y.I. Ryskin, in V.C. Farmer (Ed.), The Infrared Spectra of Minerals, Mineralogical Society, London, 1974, p. 137.
15 R.M. Potter and G. Rossman, Am. Miner., 64 (1979) 1199.
16 F. Elasass and D. Olivier, Clay Miner., 13 (1978) 299.
17 H.H.W. Moenke, in V.C. Farmer (Ed.), The Infrared Spectra of Minerals, Mineralogical Society, London, 1974, p. 365.
18 V.C. Farmer (Ed.), The Infrared Spectra of Minerals, Mineralogical Society, London, 1974.
19 P. Halbach, C. Scherhag, U. Hebisch and V. Marchig, Miner. Deposita, 16 (1981) 59.
20 D.S. Cronan and J.S. Tooms, Deep Sea Res., 16 (1969) 335.
21 G.P. Glasby, Mar. Geol., 13 (1972) 57.